Glycobiology, 2020, vol. 30, no. 3, 143–151
doi: 10.1093/glycob/cwz088
Advance Access Publication Date: 6 October 2019
Original Article

Analytical Glycobiology

Structural analysis of urinary glycosaminoglycans from healthy human subjects

Xiaorui Han[2,†], Patience Sanderson[3,†], Sara Nesheiwat[2], Lei Lin[2], Yanlei Yu[2], Fuming Zhang[2], I Jonathan Amster[3] and Robert J Linhardt[2,1]

[2]Departments of Chemistry and Chemical Biology, Biology, Chemical and Biological Engineering and Biomedical Engineering, Center for Biotechnology and Interdisciplinary Studies, Rensselaer Polytechnic Institute, 110 8th Street, Troy, NY 12180, USA and [3]Department of Chemistry, University of Georgia, 140 Cedar St, Athens, GA 30602, USA

[1]To whom correspondence should be addressed: Tel: +1-518-276-340; Fax: +1-518-276-3405; e-mail: linhar@rpi.edu
[†]X.H. and P.S. contributed equally to this work.

Received 8 July 2019; Revised 7 October 2019; Editorial Decision 9 October 2019; Accepted 9 October 2019

Abstract

Urinary glycosaminoglycans (GAGs) can reflect the health condition of a human being, and the GAGs composition can be directly related to various diseases. In order to effectively utilize such information, a detailed understanding of urinary GAGs in healthy individuals can provide insight into the levels and structures of human urinary GAGs. In this study, urinary GAGs were collected and purified from healthy males and females of adults and young adults. The total creatinine-normalized urinary GAG content, molecular weight distribution and disaccharide compositions were determined. Using capillary zone electrophoresis (CZE)–mass spectrometry (MS) and CZE–MS/MS relying on negative electron transfer dissociation, the major components of healthy human urinary GAGs were determined. The structures of 10 GAG oligosaccharides representing the majority of human urinary GAGs were determined.

Key words: capillary zone electrophoresis, glycosaminoglycans, mass spectrometry, negative electron transfer dissociation, urine

Introduction

Urine is a biofluid generated by the kidneys that collects in the bladder and is then excreted through the urethra. Kidneys function as a blood filtration system in the human body. They excrete excess water and soluble metabolism byproducts from the bloodstream, such as nitrogenous waste from amino acid and nucleic acid metabolism (urea and uric acid), and creatinine from muscle metabolism (Echeverry et al. 2010; Bouatra et al. 2013). Kidneys also help our body maintain a stable internal environment by extracting glucose to regulate blood sugar levels, by removing excess ions to maintain electrolyte (sodium, calcium, phosphorus, potassium, magnesium, chloride, bicarbonate and phosphates) balance and also by removing toxins, hormones and other waste products from blood (Bouatra et al. 2013).

Since urine contains the majority of water-soluble waste products from the human metabolism system and blood regulatory system, the chemical composition of these byproducts can provide valuable information indicative of human health. Modern clinic urinalysis is one of the most common medical diagnostic methods. The major target parameters of urinalysis include the amounts of ions and trace metals, proteins and enzymes, blood cells and glucose. Among these analytes, glucose is a particularly important indicator of diabetes mellitus (Armstrong 2007). Recent developments in medical science have shown other diseases that can be diagnosed or monitored through the types and amount of urinary glycans. Mucopolysaccharidoses (MPSs), a group of lysosomal storage disorders caused by lack of enzymes for glycosaminoglycan (GAG) metabolism, are one such disease family identified through the presence of urinary GAGs (Lehman et al. 2011; Coutinho et al. 2012). MPS results in a large increase of GAG concentration in the urine, such as heparan sulfate (HS) and keratan sulfate (KS) (Spranger et al. 2018).

GAGs in this easily accessed biofluid can be used to detect and monitor kidney pathogenesis (Gatto et al. 2016), bladder disease (Atahan et al. 1996) and metastatic prostatic cancer (Klerk and Werely 1986; Guelfi 2015). Urinary GAG analysis has been helpful in understanding glomerular-related disease (Wiggins et al. 2006), interstitial cystitis (Lose and Fransden 1990), sepsis severity (Zhang et al. 2019) and urinary tract infection (Taganna et al. 2011). In most of these pathologies, there is a large increase in the concentration of urinary GAGs simplifying their analysis. However, in the urine of healthy individuals, GAG levels are generally quite low (μg/mL levels), making their analysis quite difficult.

The total healthy human urinary GAGs have been quantified by various methods, including dimethylmethylene blue colorimetric dye-binding analysis (Alonso-Fernández et al. 2010; Dave et al. 2014), gel electrophoresis with silver staining (Al-Hakim et al. 1991; Mu et al. 2012), cetylpyridinium chloride precipitation methods (Gallegos-Arreola et al. 2000) and using ELISA kits for certain human GAGs (Mashima et al. 2016). Disaccharide analysis of human urinary GAGs has been studied by 2-aminoacridine (AMAC)-derivatized capillary electrophoresis–laser-induced fluorescence (CE–LIF) (Chang et al. 2013; Sanderson et al. 2018), and liquid chromatography–tandem mass spectrometry (LC–MS/MS) by multiple reaction monitoring (MRM) (Sun, Li, et al. 2015). The results of these different measurements resulted similar conclusions that the amount of GAG in healthy human urine was relatively low (μg/mL levels) and showed a high individual variability. The observed differences in total GAG amount were not gender-specific but varied somewhat based on an individual's age. The majority of urinary GAGs were chondroitin sulfate (CS) (on average, over 70%), followed by HS (10–30% based on detection method). Trace amounts of dermatan sulfate (DS) and hyaluronic acid (HA) were also reported.

However, because of technical limitations in the analysis of the small quantities of GAGs in the urine of healthy individuals, little, if any, detailed structural analysis has been performed on urinary GAGs. Molecular weight distribution of urinary GAGs has been previously studied by electrophoresis. However, in most of the studies, GAGs from healthy human urine only functioned as a control to MPS or other disease-affected patients' urine samples (Maccari et al. 2003; Tanyalcin, 2015). Specifically, there has been no study on the molecular weight distributions, GAG compositions or sequence of the GAGs present in healthy human urine detailed. A high-sensitivity, information-rich analytical technique is required for such detailed structural analysis. Separation is also paramount to adequately investigate complex biological samples, such as urinary GAGs. High-resolution SEC method can also achieve a robust separation efficiency and resolution (Zhang et al. 2013). Due to the highly ionic nature of sulfated GAGs, capillary zone electrophoresis (CZE) is ideally suited for separation of these molecules as it separates based on size, charge and molecular shape (Campa et al. 2006; Volpi et al. 2008; Prabhakar et al. 2009; Zamfir 2016). Coupling CZE to MS provides high sensitivity and selectivity for structural characterization of sulfated GAGs (Zaia and Costello 2001, 2003; Chi et al. 2005; Laremore et al. 2009; Laremore et al. 2010). Decades of research have been performed on sulfated GAGs using various MS fragmentation techniques (Wolff et al. 2007, 2008; Bielik and Zaia 2011; Leach, Wolff, et al. 2011a; Leach et al. 2017; Klein et al. 2019). In particular, electron-based activation, such as electron detachment dissociation and negative electron transfer dissociation (NETD), has provided more informative fragment ions to determine sequence coverage (Wolff et al. 2007, 2008, 2010; Bielik and Zaia 2011; Leach, Wolff, et al. 2011a; Leach, Xiao, et al. 2011b; Leach et al. 2017). Combining NETD with online CZE-MS can simplify the analysis process for complex GAG samples, and it can also provide sequence information for the GAG species present.

MPS and other disease-related urinary GAGs have been extensively studied by various methods in the past several years, including LC–MS, CE–LIF and other advanced analytical instrumentation (Auray-Blais et al. 2012; Chang et al. 2013; Sanderson et al. 2018). But none of these studies have reported a profile of the GAGs present in healthy human urine. Furthermore, there have been no detailed structural and compositional studies on either the GAGs present in human urine from healthy individuals or MPS patients. Herein we report the first molecular weight compositional analysis on the urinary GAGs of healthy males and females isolated using gel permeation chromatography (GPC). HS and CS/DS components ranging from disaccharides to nonasaccharides are found with a range of sulfation patterns. The 10 most abundant GAG saccharides observed by CZE–MS were fragmented using NETD MS/MS to determine modification location and structural assignments.

Results and discussion

Isolation and quantification of total GAGs in human urine

Two sets of healthy male and female donors were selected—six young adults (23–25 years of age) and adults (35–45 years of age) (Table SI). Samples were first dialyzed using controlled pore dialysis membranes (MWCO 150–500 Da and 500–1000 Da to remove salt, urea and other small molecules in the urine samples without loss of GAGs or GAG oligosaccharides. Control studies using GAG disaccharide standards showed little or no disaccharide loss through MWCO 500–1000 Da even after extensive dialysis. After digestion with actinase E to degrade proteins/peptides, urinary GAGs were purified through strong anion exchange Vivapure Q Maxi H spin column.

Total GAG amounts for each urine sample were measured by disaccharide analysis based on carbazole assay and MS–MRM. The results were normalized based on creatinine concentration to normalize the hydration levels of the individual donors (Table SII). The values determined by carbazole assay showed a higher level of variation (including negative concentrations) due to the interference of this colorimetric assay due to urine color. Thus, the total GAG present as determined by GAG disaccharide analysis based on MRM–MS was used to compound GAG content that ranged from 7 to 70 μg/mL (Figure 1A). MRM–MS analysis showed the total GAG was comprised solely of HS and CS/DS with no HA or KS observed. When samples from males and females were compared (Figure 1B), on average, female urine showed higher levels of HS than male urine, at 75.7% as compared to 68.1%, respectively. In contrast, male urine showed higher average composition of CS than female urine, at 31% as compared to 24%, respectively. Both sexes, however, displayed a smaller percentage of urinary CS than HS. Despite the differences in average values, these differences were not significant. Since an individual's age can have an impact on excreted GAGs (Lee et al. 2003), we split the urine samples into two sets, M1–3*/F1–3* (young adults) and M1–3/F1–3 (adults), and compared the percentage of HS and CS in these two groups. Based on age, the urine from young adults showed a higher average percentage of HS and a lower average percentage of CS than their adult urine counterparts (Figure 1C). These differences, based on an individual's age, were just barely significant.

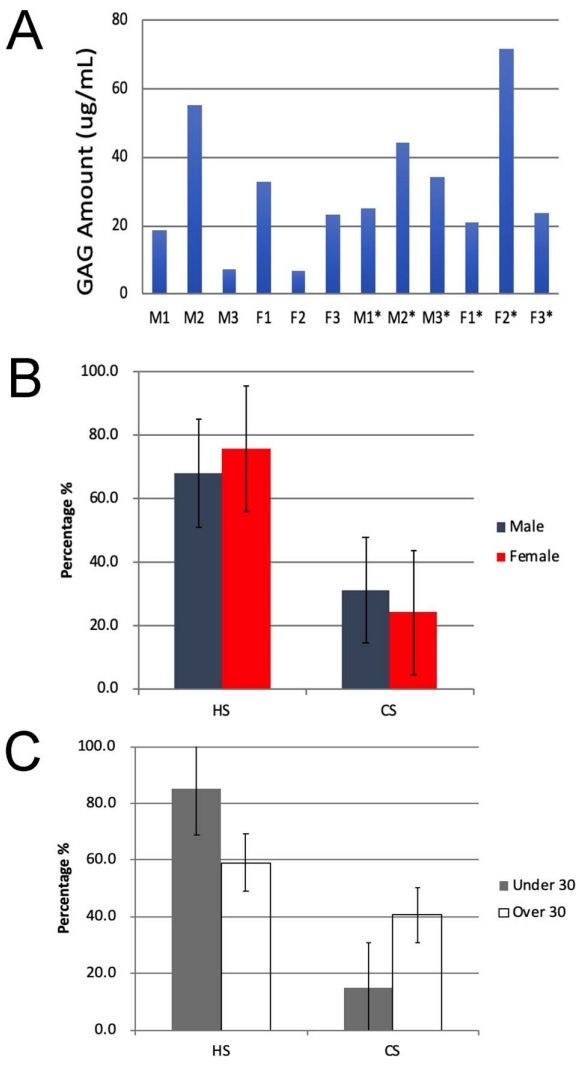

Fig. 1. Analysis of total GAG content of human urine samples. (**A**) Total GAG amount in urine sample determined through disaccharide analysis using MRM and normalized based on creatinine levels. (**B**) Comparison of HS and CS composition differences by gender in urine samples obtained from healthy male and female volunteers. (**C**) Comparison of HS and CS composition differences by age in urine samples obtained from young adults (23–25 y) and adults (35–45 y).

Disaccharide compositional analysis of GAGs in healthy human urine

The disaccharide composition of the HS and CS in each sample following enzymatic depolymerization was next determined (Table I and Table SIII). These data show that 0S was the most abundant disaccharide in the urinary HS of both males and females and in both age groups. After 0S, both male and female samples showed decreasing amounts of NS, NS2S, 6S and NS6S and TriS, respectively. Again, it should be noted that the urine from females had higher average amounts of HS disaccharides than the urine from males. The HS disaccharide composition of the urine from young adults showed a higher percentage of 0S than that from the adult group. There was less uniformity between the sexes in the disaccharide composition of CS. Female urine showed higher percentages 4S and 6S of CS disaccharides. CS of urine from young adults showed higher levels of 4S than from the urine of adults; this trend was also reflected in 4S6S, 2S4S and TriS CS disaccharides. This observation is consistent with an understanding that cartilage (comprised primarily of chondroitin 6S) breakdown increases with an individual's age (Li et al. 2013). In both age groups, 4S showed the highest levels, followed by 6S. There is a general higher sulfation level in the CS from urine samples obtained from adults compared to young adults. This is also consistent with the increased sulfation of cartilage CS with age (Lauder et al. 2001). The high level of variability in the disaccharide composition in individuals makes it difficult to draw strong conclusions as to the overall significance of these observed differences.

Molecular weight determination of urinary GAGS

The molecular weight properties of the 12 urinary GAG samples were next examined by electrophoresis on 15% polyacrylamide gels (Figure 2A and B). These gels qualitatively show similar molecular distributions for all 12 samples that can be broken into three major components—high molecular weight (top third of each lane above the degree of polymerization [dp]~20 standard), intermediate molecular weight (middle third at the dp~20 standard) and low molecular weight (lower third at and below the dp~10 standard). Nearly all of the urine samples show a band between the dp~20 and dp~10 bands. The sharpness and relative intensity of this band suggests that it may not be a GAG or GAG oligosaccharide but rather a highly charged metabolite (such as sulfated steroids) or xenobiotic generally present in urine. Two representative samples, M2* and F2*, containing sufficiently high levels of GAGs for analytical and preparative GPC, were used to more quantitatively examine molecular weight distributions by GPC using refractive index detection and are shown in Figure 2C. The high molecular weight components are shown in the void volume by the small peak at 17–20 min. The intermediate molecular weight components at 25–32 min, corresponding to the size of heparin (MW_{avg} 19 kDa), can be observed as a small broad peak. The low molecular weight components at 33–40 min, corresponding to (or smaller than) a low-molecular-weight heparin (MW_{avg} 4–5 kDa) can be observed as a large broad peak. These major low molecular weight components were analyzed by CZE–MS/MS.

CZE–MS analysis of low-molecular-weight human urinary GAGs

The high sensitivity of CZE–MS allows detection and separation of GAGs at low concentrations to determine various GAG compositions in urine. The low molecular weight components (MW < 5 kDa) recovered by GPC from two of the urine samples, M2* and F2*, were analyzed using CZE–MS/MS. After reconstituting these low-molecular-weight GAG components from the GPC fractions in 30 µL of water, they were separated by CZE–MS. A variety of compositions were determined by extracting the m/z and charge of the ions and using in-lab automated software developed for assignment (Duan and Amster 2018).

The majority of the species identified in the M2* and F2* samples were similar, with GAG chains ranging in size from dp2 to dp9 containing both HS and CS/DS components (Figure 3). The M2* sample was at a higher concentration and resulted in detection of 81 different compositions while the lower amount of the F2* contained only 28 compositions. The variability between the compositions comprising the M2* and F2* samples is shown in Figure 3A. Pentasaccharides were the most abundant chain lengths with 17 different compositions

Table I. HS and CS compositional analysis

HS disaccharide composition (mole %)								
Disaccharide	TriS	NS6S	NS2S	NS	2S6S	6S	2S	0S
Range (μg/mL)	0–0.35	0.11–2.66	0.14–3.06	0.37–6.47	0–0.02	0.16–2.64	0–0.21	2.94–30.57
Mean (μg/mL)	0.14	0.68	0.91	2.39	0	0.92	0.05	13.17
SD	0.11	0.83	0.80	1.90	0.01	0.71	0.06	9.58
CS disaccharide composition (mole %)								
Disaccharide	TriS	2S4S	2S6S	4S6S	4S	6S	2S	0S
Range (μg/mL)	0–2.28	0.13–2.14	0.08–0.85	0.12–4.01	3.37–27.36	0.54–13.96	0.01–1.52	0.22–2.86
Mean (μg/mL)	0.20	0.73	0.42	1.21	11.46	2.85	0.27	1.12
SD	0.66	0.59	0.27	1.10	8.51	3.75	0.42	0.93

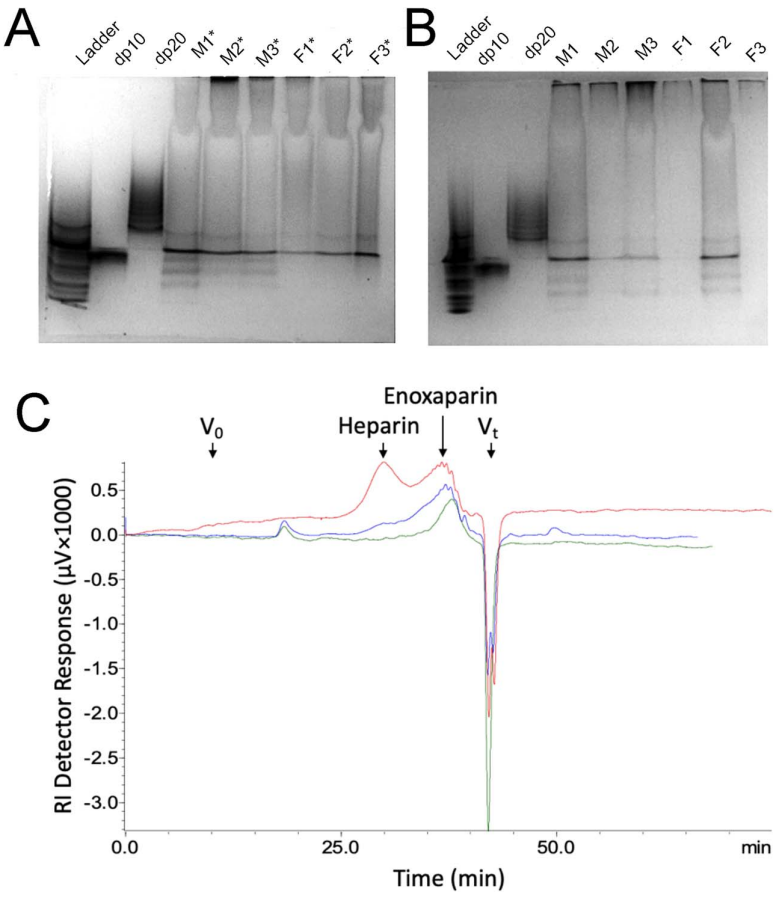

Fig. 2. Molecular weight distribution of human urinary GAGs. (**A** and **B**) show PAGE results on 15% gel stained with alcian blue and imaged with Biorad gel imaging software. Samples were from young adults (M1*, M2*, M3*, F1*, F2*, F3*) in gel A and from young adults (M1, M2, M3, F1, F2, F3) in gel B. Standards run in each gel include a ladder of oligosaccharides prepared from the partial digestion of bovine lung heparin (Edens et al. 1992). The dp∼10 (MW_{avg} 3325) and dp∼20 (MW_{avg} 6650) standards were prepared by fractionating bovine lung heparin oligosaccharides by low-pressure GPC (Edens et al. 1992). (**C**) Shows the GPC analysis using refractive index detection of two urine samples M2* (blue trace) and F2* (green trace). A mixture of unfractionated heparin (MW_{avg} 19,000) and enoxaparin (a low-molecular-weight heparin, MW_{avg} 4500) are shown as standards (red trace).

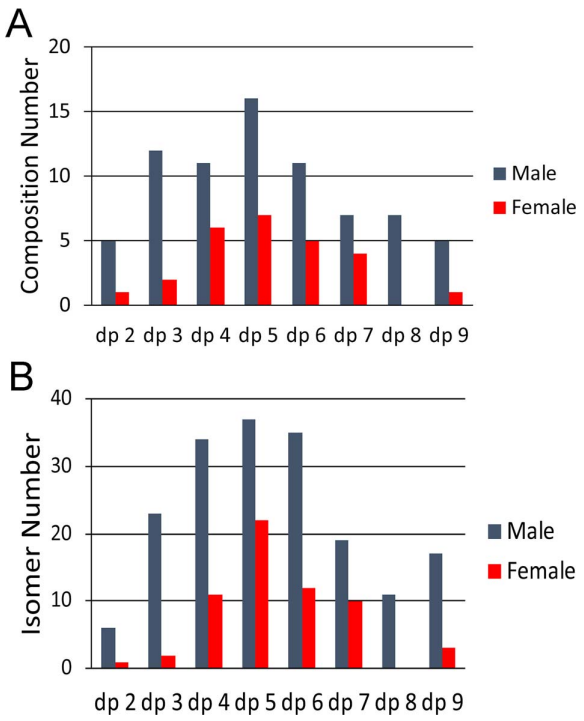

Fig. 3. Comparison of the sulfated GAGs recovered from urine coming from a healthy, young adult male (M2*) and female (F2*) individual. (**A**) Composition matches of varying chain lengths containing both HS and CS/DS. (**B**) Amount of isomers detected for each dp.

for M2* and 7 for F2*. Urine is a complex biological sample with a multitude of GAGs present. Thus, after composition analysis, each GAG precursor was manually interrogated to determine the number of isomers present in the samples (Figure 3B). As expected, based on the compositional information, the number of isomers was higher for M2* (158) than for F2* (60) sample with dp4–6 representing the largest number of isomers present for both sexes. The composition and isomer components are provided in the Supplementary data (Table SIV).

Of particular interest are the structures found in Peaks 1 and 3–5 (Figure 4) as these suggest the presence of an unsaturated (−18 amu) ΔUA residue at the nonreducing end of these four HS oligosaccharides. Such ΔUA residues are commonly observed on the treatment of GAGs with a microbial polysaccharide lyase, but such enzymes are not found in mammals (Linhardt et al. 1986). A heparin lyase has been isolated from the human colonic bacterium, *Bacillus stercoris* (Ahn et al. 1998), suggesting that these HS oligosaccharides might have a dietary source.

CZE–MS/MS analysis of low-molecular-weight human urinary GAGs

Further investigation into the sample relied on online MS/MS experiments. By combining NETD experiments with CZE–MS, the top 10 most abundant species in both the M2* and F2* samples were structurally analyzed. The CZE separations are shown in their extracted ion EIEs (Figure 4). The EIEs of both samples are strikingly similar showing the same set of peaks at similar relative intensities, but the M2* with a higher concentration showed higher abundance of GAGs when using the same conditions and injection volumes. The 10 most abundant GAG precursor mass values extracted from the low-molecular-weight GAGs from F2* (Figure 4A) and M2* (Figure 4B) urine are identified. The structures provided were determined using NETD MS/MS, and they are the same for both sexes designated by the peak number.

The NETD mass spectrum of a trisaccharide containing five sulfo groups is displayed in Figure 5. This HS trisaccharide is the second GAG to migrate through the capillary (Peak 2, Figure 4, A and B). The averaged NETD MS/MS spectrum is from M2* at 20.89 min, but the corresponding F2* Peak 2 mass spectrum looks similar. Fragment ions are depicted using the Domon–Costello nomenclature. Glycosidic cleavages are the most abundant fragments aside from the neutral losses. The glycosidic cleavages in addition to the mass of the precursor enable assignment of the *N*-sulfo modification on the hexosamine residues. In addition, the glycosidic cleavages indicate the hexosamine residues have two sulfo groups with the uronic acid containing a single sulfo group. While it is not possible to determine the stereochemistry of *C*-5 on the acidic sugar, it is represented by a white diamond with the sulfate located at the 2-*O* position. There are three cross-ring assignments represented by red boxes ($^{1,5}X_2$, $^{2,5}X_2$ and $^{0,2}A_3$). The cross-ring assignments occur on the hexosamines, but do not distinguish between 6-*O* and 3-*O* sulfation on these residues. Thus, the sulfo groups might be in either the 3-*O* or 6-*O* position and are represented as "S" on the structure in Figure 5. The structure based on human HS biosynthesis most likely corresponds to GlcNS6S (1 → 4) IdoA2S (1 → 4) GlcNS6S. The remaining GAG species from F2* and M2* can be found in the Supplementary data (Table SIV).

From the fragmentation patterns, it was possible to identify that residues contain sites of modification, such as sulfation or *N*-acetylation, for each polysaccharide. Additionally, separation and characterization of positional isomers was accomplished on dp7 carbohydrates with three different sulfation patterns (Figure 4A and B, Peaks 6–8). The five peaks that migrate through the capillary first appear to potentially be HS species based on the number of sulfo modifications in addition to the presence of abundant of *N*-sulfation. The latter five species appear to be CS/DS based on the moderate sulfation patterns (one per disaccharide) and number of *N*-acetyl group present. However, this is not confirmed at this time so the hexosamines are presented by white squares if they do not contain *N*-sulfation. Further analysis will be required to more completely delineate these structures.

Although it was not possible to distinguish between 6-*O* from 3-*O* sulfation for HS (and the 4-*O* from the 6-*O* sulfation for CS/DS), the number of sulfo modifications on sugar residues was determined for 10 sulfated GAGs. The most abundant GAG species found in both samples was a disaccharide with three sulfo modifications. Overall, the abundance was higher for M2* compared to F2*, but both samples had similar profiles and compositions for the 10 most abundant GAGs. The variation in the number of compositions and isomers could be a result of the concentration difference between the samples.

Conclusions

A detailed structural and compositional GAGs profile of health urinary GAGs was reported in this study. Urinary GAGs collected and purified from individuals of different age (young adults under 30 and adults over 30) and from males and females were analyzed in this work. The total creatinine-normalized GAG concentrations

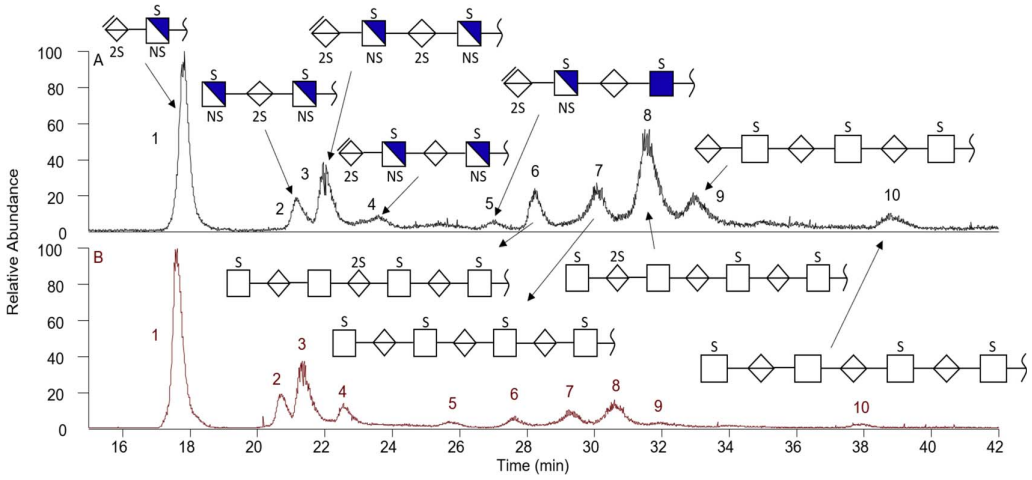

Fig. 4. Extracted ion EIEs from the CZE–MS analysis of the 10 most abundant GAG oligosaccharides recovered from the urine of healthy, young adult donors. (**A**) EIE of the major low-molecular-weight GAGs recovered from the urine of a female donor, F2*. (**B**) EIE of the major low-molecular-weight GAGs recovered from the urine of a male donor, M2*. Structures were determined using NETD MS/MS (as shown in Figure 5) are the same for both sexes designated by the peak number.

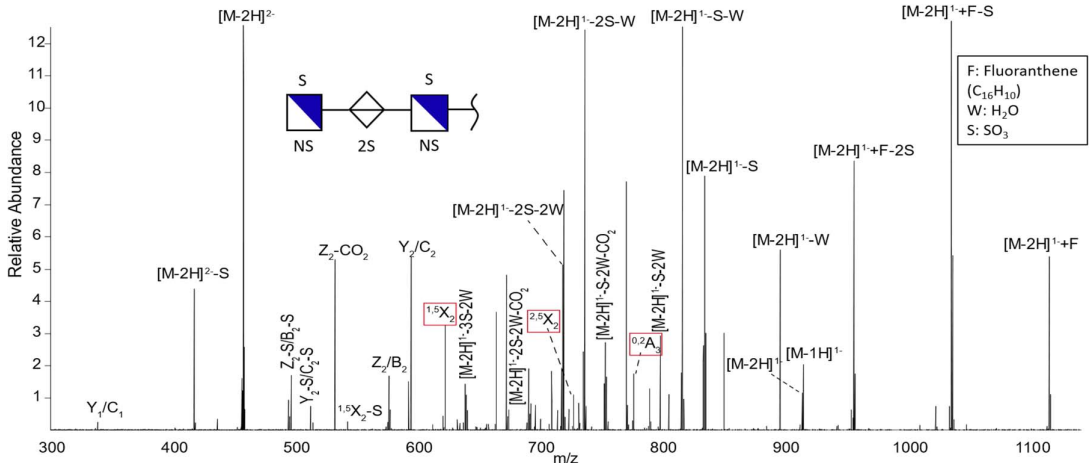

Fig. 5. NETD tandem mass spectrum of Peak 2 at 20.89 min (Figure 4) corresponding to a HS trisaccharide containing five sulfate groups is shown. The boxes in red indicate the cross-ring cleavages.

ranged from 7 to 70 μg/mL. HS was the most prominent urinary GAG followed by CS and no HA and KS were detected. Disaccharide compositional analysis based on LC–MS MRM showed that 0S is the predominant HS disaccharide and 4S was the predominant CS disaccharide. Molecular weight analysis suggested the presence of intact GAGs as well as GAG oligosaccharides with the majority of urinary GAGs being oligosaccharides of chain sizes from dp2–20. Urine from males had slightly more CS and urine samples collected from young adults have a higher percentage HS. The CZE–MS/MS analysis of urinary GAG oligosaccharides from two samples for urine collected from a healthy young adult male and female gave similar profiles having the same 10 most abundant GAG oligosaccharides. Interestingly, four of these oligosaccharides contain ΔUA residues at their nonreducing end suggesting they might originate from dietary sources. Since this study examines only a relatively small number of nondiverse individuals who are not controlled for controls for diet, hydration level nor individually evaluated for health, the results presented do not define the "normal" ranges of GAG concentration and structure but instead represent only typical values in healthy individuals. Additional well-controlled clinical studies will be required to set "normal" ranges of GAG concentration and structure.

Materials and methods

Materials

All chemicals and reagents were obtained from commercial sources and used as received unless otherwise specified. Healthy human urine samples from healthy males and six healthy females were purchased from BioreclamationIVT (Westbury, NY) (see Table SI). No information on protection of human subjects was required for this study based on National Institute of Health guidelines, as unidentified biospecimens from living individuals obtained from a commercial provider are not considered human subjects research. Seventeen unsaturated HA, HS and CS disaccharide standards were purchased

from Iduron (Cheshire, UK). Actinase E was from KaKen Biochemicals (Tokyo, Japan). Recombinant *Flavobacterium heparinum* heparin lyases I, II and III; *Proteus vulgaris* chondroitin lyase ABC; and keratanase II were expressed in *Escherichia coli* and purified in our laboratory as previously described. Keratanase 1 from *Pseudomonas sp*. was obtained from Sigma (St. Louis, MO). TSK gel 3000 SWxl and 4000 SWxl were from Tosoh Bioscience (King of Prussia, PA). BFS capillaries (360 µm OD × 50 µm ID) were purchased from PolyMicro Technologies (Phoenix, AZ), and coated electrospray emitters (1.0 mm OD × 0.75 mm ID, E-BS-CC1-750-1000-10 µ-B30) were obtained from CMP Scientific (Brooklyn, NY). Coating reagent *N*-(6-aminohexyl) aminomethyltriethoxysilane (Gelest, Morrisville, PA) was prepared in toluene and applied to the capillary as previously described (Sanderson et al. 2018). Dialysis membranes were from Spectrum Chemical (New Brunswick, NJ).

Sample preparation

Urine samples were defrosted at 4°C and mixed well using a vortex mixer. 80 mL of each sample was used for GAG preparation. Small molecules and salts were removed by dialysis (molecular weight cut-off [MWCO] 150–500 Da) against distilled water and then freeze-dried to recover the crude GAGs. All lyophilized crude urinary GAGs were suspended in 10 mL of water, proteolyzed at 55°C with 10 mg/mL actinase E for 24 h, and the mixture was then lyophilized. The lyophilized samples were dissolved in 5 mL of a solution of denaturing buffer (8 M urea containing 2% wt. CHAPS), bound to a Vivapure Q Maxi H spin column, washed twice with 10 mL of denaturing buffer and washed three times with 10 mL of 0.2 M NaCl. The GAG components were then eluted from the spin column with three 10 mL volumes of 16% NaCl, and the salt in these fractions was removed by exhaustive dialysis (MWCO 500–1000 Da) against distilled water and freeze-dried to recover the purified GAGs.

Disaccharides analysis

Purified urinary GAGs (approximately 5 µg) were dissolved in 300 µL of digestion buffer (50 mM ammonium acetate, 2 mM calcium chloride). Recombinant heparin lyase I, II and III; chondroitin lyase ABC; and keratanase I and II (10 mU of each enzyme) were then added to the reaction buffer and placed in a 37°C incubator overnight. The disaccharides were recovered by passing through a 3000 Da MWCO spin column. The filter unit was washed twice with 200 µL of distilled water, and the combined fractions were finally lyophilized. The dried samples were labeled with AMAC by adding 10 µL of 0.1 M AMAC in dimethyl sulfoxide/acetic acid (17/3, v/v) incubating at room temperature (RT) for 10 min, followed by adding 10 µL of 1 M aqueous sodium cyanoborohydride and incubating for 1 h at 45°C. The resulting samples were centrifuged at 13,200 rpm for 20 min. Supernatant was collected and analyzed by HPLC–MS on an Agilent 1200 LC/MSD instrument (Agilent Technologies, Inc. Wilmington, DE) equipped with a 6300 ion trap and a binary pump. The column used was a Poroshell 120 C18 column (3.0 × 50 mm, 2.7 µm, Agilent) at 45°C. Eluent A was 50 mM ammonium acetate solution, and eluent B was methanol. The mobile phase passed through the column at a flow rate of 250 µL/min with 10 min linear gradients of 10–35% solution B. The electrospray interface was set in negative ionization mode with a skimmer potential of −40.0 V, a capillary exit of −40.0 V and a source temperature of 350°C to obtain the maximum abundance of the ions in a full-scan spectrum (300–850 Da). Nitrogen (8 L/min, 40 psi) was used as a drying and nebulizing gas.

Molecular weight distribution of urinary GAGs using polyacrylamide gel electrophoresis

Polyacrylamide gel electrophoresis (PAGE) was used to determine the molecular weight distribution of GAGs. The purified urinary GAGs were separated by a 15% total acrylamide, containing 14.08% (w/v) acrylamide, 0.92% (w/v) *N,N*-methylene-bis-acrylamide and 5% (w/v) sucrose. The acrylamide monomer solutions were prepared in resolving buffer (0.1 M boric acid, 0.1 M TriS, 0.01 M disodium ethylenediaminetetraacetic acid, pH 8.3). Stacking gel monomer solution was prepared in resolving buffer, containing 4.75% (w/v) acrylamide and 0.25% (w/v) *N,N*-methylene-bis-acrylamide, and the pH was adjusted to 6.3 using hydrochloric acid (HCl). A 10 cm × 7 mm diameter resolving gel column was cast from 4 mL of 15% resolving gel solution containing 4 µL of tetramethylethylenediamine and 12 µL of 10% ammonium persulfate. A stacking gel was cast from 1 mL of stacking gel monomer solution containing 1 µL of tetramethylethylenediamine and 30 µL of 10% ammonium persulfate. Phenol red dye was added to the sample for visualization of the ion front during electrophoresis. In each lane, ∼5 µg of sample was subjected to electrophoresis. A standard composed mixture of heparin oligosaccharides with known molecular weights was prepared enzymatically from bovine lung heparin (Edens et al. 1992). The gel was visualized with alcian blue staining and then digitized with UN-SCAN-IT to estimate molecular weight.

Molecular weight distribution of urinary GAGs using GPC

Oligosaccharides separated by size exclusion column (Tosoh Bioscience TSKgel G3000SWxl and TSKgel G4000SWxl columns) with online differential refraction detector. Mobile phase was 50 mM ammonium acetate at 0.5 mL/min. GAGs were extracted by performing dialysis and treatment with actinase E to remove proteins on a Mini Q cation column. Recovered GAGs were subjected to GPC to obtain low-molecular-weight oligosaccharides before reconstituting in water for CZE–MS analysis.

CZE–MS/MS of oligosaccharides

CZE separations were performed on an Agilent HP 3D CE instrument using a cation-coated capillary with a –30 kV potential applied. Ammonium acetate (25 mM in 70% methanol) was used as the background electrolyte and sheath liquid to provide reproducible separations and optimal spray stability. Conditions and parameters were consistent with previously reported literature used for purified GAG standards (Sanderson et al. 2018). Samples were injected for 9 s at 950 mbar followed by a BGE injection for 10 s at 10 mbar.

An EMASS-II (CMP Scientific) CE–MS interface was employed to couple the CE with a Thermo Scientific (Bremen, Germany) Velos Orbitrap Elite mass spectrometer (Sun, Zhu, et al. 2015; Lin et al. 2017). The etched capillary outlet was nested inside of a cation-coated glass emitter tip with a 30 µm tip orifice. The etched capillary was positioned 0.3–0.5 mm from the tip of the emitter orifice to create a mixing volume of ∼15 nL that was filled with sheath liquid. Nanoelectrospray ionization voltage was applied by an external power supply ranging from −1.85 to −1.9 kV to the emitter.

MS detection was performed in negative-ion mode, and multiply-deprotonated anions were observed for each species. Sucrose octasulfate was utilized prior to CZE–MS experiments to perform a semi-automatic optimization of source parameters. This improved sensitivity of sulfated GAGs and decreased sulfate loss during MS analysis. The Orbitrap was scanned from m/z 150–2000 for GAG

oligosaccharides with a specified resolution of 120,000 for MS and MS/MS experiments. MS/MS experiments were performed using NETD MS/MS with fluoranthene as the reagent cation for activation. Mass selection of the precursors occurred in the dual linear ion trap. Activation with fluoranthene for doubly and triply charged precursors was ~125 ms and ~50 ms, respectively. Each peak from the electropherogram (EIE) was averaged to obtain a tandem mass spectrum with mass accuracy of 10 ppm or better. Data analysis was performed using Glycoworkbench (Ceroni et al. 2008) and in-lab developed software (Duan and Amster 2018). Fragments were assigned based on the Domon–Costello nomenclature (Domon and Costello 1988).

Supplementary data

Supplementary data for this article is available online at http://glycob.oxfordjournals.org/.

Funding

National Institutes of Health—grants (CA231074), (DK111958), (HL136271), (HL125371) and (GM103390).

Conflict of interest statement

None declared.

References

Ahn MY, Shin KH, Kim D-H, Jung E-A, Toida T, Linhardt RJ, Kim YS. 1998. Characterization of *Bacteroides* species from human intestine that degrades glycosaminoglycans. *Can J Microbiol*. 44:423–429.

Al-Hakim A, Linhardt RJ. 1991. Electrophoresis and detection of nanogram quantities of exogenous and endogenous glycosaminoglycans in biological fluids. *Appl Theor Electrophor*. 1:305–312.

Alonso-Fernández J, Fidalgo J, Colón C. 2010. Neonatal screening for mucopolysaccharidoses by determination of glycosaminoglycans in the eluate of urine-impregnated paper: Preliminary results of an improved DMB-based procedure. *J Clin Lab Anal*. 24(3):149–153.

Armstrong J. 2007. Urinalysis in Western culture: A brief history. *Kidney Int*. 71(5):384–387.

Atahan Ö, Kayigil Ö, Hizel N, Yavuz Ö, Metin A. 1996. Urinary glycosaminoglycan excretion in bladder carcinoma. *Scand J Urol Nephrol*. 30(3):173–177.

Auray-Blais C, Lavoie P, Zhang H, Gagnon R, Clarke JT, Maranda B, Young SP, An Y, Millington DS. 2012. An improved method for glycosaminoglycan analysis by LC–MS/MS of urine samples collected on filter paper. *Clin Chim Acta*. 413(7–8):771–778.

Bielik AM, Zaia J. 2011. Multistage tandem mass spectrometry of chondroitin sulfate and dermatan sulfate. *Int J Mass Spectrom*. 305(2–3):131–137.

Bouatra S, Aziat F, Mandal R, Guo AC, Wilson MR, Knox C, Bjorndahl TC, Krishnamurthy R, Saleem F, Liu P *et al*. 2013. The human urine metabolome. *PLoS One*. 8(9):e73076.

Campa C, Coslovi A, Flamigni A, Rossi M. 2006. Overview on advances in capillary electrophoresis–mass spectrometry of carbohydrates: A tabulated review. *Electrophoresis*. 27(11):2027–2050.

Ceroni A, Maass K, Geyer H, Geyer R, Dell A, Haslam SM. 2008. GlycoWorkbench: A tool for the computer-assisted annotation of mass spectra of glycans. *J Proteome Res*. 7(4):1650–1659.

Chang Y, Yang B, Weyers A, Linhardt RJ. 2013. Capillary electrophoresis for the analysis of glycosaminoglycan-derived disaccharides. *Methods Mol Biol*. 984:67–77.

Chi L, Amster J, Linhardt RJ. 2005. Mass spectrometry for the analysis of highly charged sulfated carbohydrates. *Curr Anal Chem*. 1(3):223–240.

Coutinho MF, Lacerda L, Alves S. 2012. Glycosaminoglycan storage disorders: A review. *Biochem Res Int*. 2012:1–16.

Dave MB, Chawla PK, Dherai AJ, Ashavaid TF. 2014. Urinary glycosaminoglycan estimation as a routine clinical service. *Indian J Clin Biochem*. 30(3):293–297.

Domon B, Costello CE. 1988. A systematic nomenclature for carbohydrate fragmentations in FAB-MS/MS spectra of glycoconjugates. *Glycoconj J*. 5(4):397–409.

Duan J, Amster IJ. 2018. An automated, high-throughput method for interpreting the tandem mass spectra of glycosaminoglycans. *J Am Soc Mass Spectrom*. 29(9):1802–1811.

Echeverry G, Hortin GL, Rai AJ. 2010. Introduction to urinalysis: Historical perspectives and clinical application. *Methods Mol Biol*. 641:1–12.

Edens RE, Al-Hakim A, Weiler JM, Rethwisch DG, Fareed J, Linhardt RJ. 1992. Gradient polyacrylamide gel electrophoresis for determination of the molecular weights of heparin preparations and low-molecular-weight heparin derivatives. *J Pharm Sci*. 81:823–827.

Gallegos-Arreola MP, Machorro-Lazo M, Flores-Martínez Silvia E, Zúñiga-González GM, Figuera LE, González-Noriega A, Sánchez-Corona J. 2000. Urinary glycosaminoglycan excretion in healthy subjects and in patients with mucopolysaccharidoses. *Arch Med Res*. 31(5):505–510.

Gatto F, Maruzzo M, Magro C, Basso U, Nielsen J. 2016. Prognostic value of plasma and urine glycosaminoglycan scores in clear cell renal cell carcinoma. *Front Oncol*. 6:253.

Guelfi G. 2015. Characterization of kallireins and microRNAs in urine sediment for the discrimination of prostate cancer from benign prostatic hyperplasia. *J Cancer Sci Ther*. 07(04):130–136.

Klein DR, Leach FE III, Amster IJ, Brodbelt JS. 2019. Structural characterization of glycosaminoglycan carbohydrates using ultraviolet photodissociation. *Anal Chem*. 91(9):6019–6026.

Klerk DPD, Werely C. 1986. Urinary glycosaminoglycan excretion in metastatic prostate cancer. *World J Urol*. 4(4):200–204.

Laremore TN, Leach FE, Solakyildirim K, Amster IJ, Linhardt RJ. 2010. Glycosaminoglycan characterization by electrospray ionization mass spectrometry including Fourier transform mass spectrometry. *Methods Enzymol*. 478:79–108.

Laremore TN, Zhang F, Dordick JS, Liu J, Linhardt RJ. 2009. Recent progress and applications in glycosaminoglycan and heparin research. *Curr Opin Chem Biol*. 13(5):633–640.

Lauder RM, Huckerby TN, Brown GM, Bayliss MT, Nieduszynski IA. 2001. Age-related changes in the sulphation of the chondroitin sulphate linkage region from human articular cartilage aggrecan. *Biochem J*. 358:523–528.

Leach FE, Riley NM, Westphall MS, Coon JJ, Amster IJ. 2017. Negative electron transfer dissociation sequencing of increasingly sulfated glycosaminoglycan oligosaccharides on an Orbitrap mass spectrometer. *J Am Soc Mass Spectrom*. 28(9):1844–1854.

Leach FE, Wolff JJ, Xiao Z, Ly M, Laremore TN, Arungundram S, Al-Mafraji K, Venot A, Boons G-J, Linhardt RJ *et al*. 2011a. Negative electron transfer dissociation Fourier transform mass spectrometry of glycosaminoglycan carbohydrates. *Eur J Mass Spectrom (Chichester)*. 17(2):167–176.

Leach FE, Xiao Z, Laremore TN, Linhardt RJ, Amster IJ. 2011b. Electron detachment dissociation and infrared multiphoton dissociation of heparin tetrasaccharides. *Int J Mass Spectrom*. 308(2):253–259.

Lee EY, Kim SH, Whang SK, Hwang KY, Yang JO, Hong SY. 2003. Isolation, identification, and quantitation of urinary glycosaminoglycans. *Am J Nephrol*. 23:152–157.

Lehman TJA, Miller N, Norquist B, Underhill L, Keutzer J. 2011. Diagnosis of the mucopolysaccharidoses. *Rheumatology*. 50(Suppl 5):v41–v48.

Li Y, Wei X, Zhou J, Wei L. 2013. The age-related changes in cartilage and osteoarthritis. *Biomed Res Int*. 2013:916530.

Lin L, Liu X, Zhang F, Chi L, Amster IJ, Leach FE, Xia Q, Linhardt RJ. 2017. Analysis of heparin oligosaccharides by capillary electrophoresis–negative-ion electrospray ionization mass spectrometry. *Anal Bioanal Chem*. 409(2):411–420.

Linhardt RJ, Galliher PM, Cooney CL. 1986. Polysaccharide Lyases. *Appl Biochem Biotechnol*. 12:135–177.

Lose G, Jespersen J, Fransden B, Højensgård JC, Astrup T. 1985. Subcutaneous heparin in the treatment of interstitial cystitis. *Scand J Urol Nephrol*. 19(1):27–29.

Maccari F, Gheduzzi D, Volpi N. 2003. Anomalous structure of urinary glycosaminoglycans in patients with pseudoxanthoma elasticum. *Clin Chem*. 49(3):380–388.

Mashima R, Sakai E, Tanaka M, Kosuga M, Okuyama T. 2016. The levels of urinary glycosaminoglycans of patients with attenuated and severe type of mucopolysaccharidosis II determined by liquid chromatography–tandem mass spectrometry. *Mol Genet Metab Rep*. 7:87–91.

Mu AK-W, Lim B-K, Hashim OH, Shuib AS. 2012. Detection of differential levels of proteins in the urine of patients with endometrial cancer: Analysis using two-dimensional gel electrophoresis and o-glycan binding lectin. *Int J Mol Sci*. 13(8):9489–9501.

Prabhakar V, Capila I, Sasisekharan R. 2009. The structural elucidation of glycosaminoglycans. *Methods Mol Biol*. 534:147–156.

Sanderson P, Stickney M, Leach FE, Xia Q, Yu Y, Zhang F, Linhardt RJ, Amster IJ. 2018. Heparin/heparan sulfate analysis by covalently modified reverse polarity capillary zone electrophoresis–mass spectrometry. *J Chromatogr A*. 1545:75–83.

Spranger JW, Brill PW, Hall C, Nishimura G, Superti-Furga A, Unger S. 2018. Mucopolysaccharidoses and oligosaccharidoses. In: *Bone dysplasias*. Oxford University Press, USA. p. 109–134.

Sun L, Zhu G, Zhang Z, Mou S, Dovichi NJ. 2015a. Third-generation electrokinetically pumped sheath-flow nanospray interface with improved stability and sensitivity for automated capillary zone electrophoresis–mass spectrometry analysis of complex proteome digests. *J Proteome Res*. 14(5):2312–2321.

Sun X, Li L, Overdier KH, Ammons LA, Douglas IS, Burlew CC, Zhang F, Schmidt EP, Chi L, Linhardt RJ. 2015b. Analysis of total human urinary glycosaminoglycan disaccharides by liquid chromatography–tandem mass spectrometry. *Anal Chem*. 87(12):6220–6227.

Taganna J, De Boer AR, Wuhrer M, Bouckaert J. 2011. Glycosylation changes as important factors for the susceptibility to urinary tract infection. *Biochem Soc Trans*. 39(1):349–354.

Tanyalcin MT. 2015. Urinary glycosaminoglycan electrophoresis with optimized keratan sulfate separation using Peltier system for the screening of mucopolysaccharidoses. *J Inborn Errors Metab Screen*. 3: 1–5.

Volpi N, Maccari F, Linhardt RJ. 2008. Capillary electrophoresis of complex natural polysaccharides. *Electrophoresis*. 29(15):3095–3106.

Wiggins JE, Goyal M, Wharram BL, Wiggins RC. 2006. Antioxidant ceruloplasmin is expressed by glomerular parietal epithelial cells and secreted into urine in association with glomerular aging and high-calorie diet. *J Am Soc Nephrol*. 17(5):1382–1387.

Wolff JJ, Amster IJ, Chi L, Linhardt RJ. 2007. Electron detachment dissociation of glycosaminoglycan tetrasaccharides. *J Am Soc Mass Spectrom*. 18(2):234–244.

Wolff JJ, Laremore TN, Busch AM, Linhardt RJ, Amster IJ. 2008. Electron detachment dissociation of dermatan sulfate oligosaccharides. *J Am Soc Mass Spectrom*. 19(2):294–304.

Wolff JJ, Leach FE, Laremore TN, Kaplan DA, Easterling ML, Linhardt RJ, Amster IJ. 2010. Negative electron transfer dissociation of glycosaminoglycans. *Anal Chem*. 82(9):3460–3466.

Zaia J, Costello CE. 2001. Compositional analysis of glycosaminoglycans by electrospray mass spectrometry. *Anal Chem*. 73(2):233–239.

Zaia J, Costello CE. 2003. Tandem mass spectrometry of sulfated heparin-like glycosaminoglycan oligosaccharides. *Anal Chem*. 75(10):2445–2455.

Zamfir AD. 2016. Applications of capillary electrophoresis electrospray ionization mass spectrometry in glycosaminoglycan analysis. *Electrophoresis*. 37(7–8):973–986.

Zhang Q, Chen X, Zhu Z, Zhan X, Wu Y, Song L, Kang J. 2013. Structural analysis of low molecular weight heparin by ultraperformance size exclusion chromatography/time of flight mass spectrometry and capillary zone electrophoresis. *Anal Chem*. 85(3):1819–1827.

Zhang X, Han X, Xia K, Xu Y, Yang Y, Oshima K, Haeger SM, Perez MJ, Mcmurtry SA, Hippensteel JA *et al*. 2019. Circulating heparin oligosaccharides rapidly target the hippocampus in sepsis, potentially impacting cognitive functions. *Proc Natl Acad Sci U S A*. 116: 9208–9213.